Materials Science & Engineering A 616 (2014) 116–122

Contents lists available at ScienceDirect

Materials Science & Engineering A

journal homepage: www.elsevier.com/locate/msea

Effect of pre-strain on hydrogen embrittlement of high strength steels

Xinfeng Li [a], Yanfei Wang [b], Peng Zhang [a], Bo Li [a], Xiaolong Song [a,*], Jing Chen [a]

[a] State Key Laboratory for Mechanical Behavior of Materials, Xi'an Jiaotong University, Xi'an 710049, China
[b] College of Mechanical and Power Engineering, Nanjing University of Technology, Nanjing 211816, China

ARTICLE INFO

Article history:
Received 5 May 2014
Received in revised form
14 July 2014
Accepted 27 July 2014
Available online 2 August 2014

Keywords:
Hydrogen embrittlement
Pre-strain
High strength steel

ABSTRACT

The effect of the pre-strain on hydrogen embrittlement (HE) of high strength steels was investigated by slow strain-rate tensile (SSRT). The specimens were electrochemically hydrogen-charged in 0.5 mol/L H_2SO_4 with 1 g/L CH_4N_2S at room temperature for 24 h. It is found that the amount of hydrogen increases linearly with the exponent of pre-strain, i.e., $C_H = 11.963 + 0.00385\exp(1.144\varepsilon_P)$. The HE susceptibility of the alloy initially decreases and then increases with increasing pre-strain. The ultimate tensile strength for the hydrogen-charged specimen is highest in the 3% pre-strain, which is interpreted by competition between strain hardening and Hydrogen Enhanced Decohesion (HEDE) mechanism. The fracture mode shows a mixed mode fracture of quasi-cleavage and intergranular fracture for hydrogen-charged specimens while the fracture mode exhibits dimples for hydrogen-free specimens.

1. Introduction

Steels often suffer from a loss of ductility and strength due to the presence of hydrogen. This phenomenon is well known as hydrogen embrittlement (HE), and has been much studied and reported. It was found that severe HE may occur in high strength steels, leading to sudden and premature failures of the steels. And generally the susceptibility to HE increases with enhancing strength level [1–4].

Due to a good durability performance in aggressive environments, prestressed concrete has been widely used since 1928. High strength steel bars are used in a prestressed concrete structure. However, premature failures of prestressed high strength steel bars caused by HE have been reported [5–7]. The possible sources of hydrogen contain corrosion, cathodic protection and galvanizing and grout.

Several documents have reported that the quantity of hydrogen increased with pre-strain [8–10]. However, the effect of pre-strain on susceptibilities of HE is a controversial issue. On the one hand, Takasugi et al. [11] reported that as the pre-deformation increased, tensile elongation of the Ni_3Al alloy increased, indicating decreased HE. They explained this as due to the trapping of hydrogen atoms to dislocations or vacancies induced by pre-deformation, and hydrogen atoms enriching grain boundaries could be reduced to a level below the critical content. In addition, A similar pre-strain effect was found in TRIP steels [12], Ni-base Ally 600 [13]. On the other hand, Hui et al. [10] revealed that for a medium-carbon TRIP steel the amount of charged hydrogen increased with increasing pre-strain, consequently hydrogen-induced ductility loss increased.

With respect to the high strength steels, the effect of pre-strain on HE has rarely been investigated. Therefore, it is necessary to study the effect of pre-strain on HE of high strength steels.

2. Experimental

2.1. Materials and specimens

Screw-thread steel bars were used in this study. After hot-rolling from 150 mm × 150 mm continuous casting billet to steel bars, the steel bars underwent air-cooling to room temperature and then tempering at 623 K for 5 h. The chemical composition of the steel bars is given in Table 1. Tensile specimens with dimensions of ⌀5 × 25 mm were machined from the bars with tensile axis parallel to the rolling direction.

2.2. Electrochemical hydrogen-charged

One group of the pre-strained specimens was electrochemically charged with hydrogen in 0.5 mol/L H_2SO_4 solution at a current density of 0.3 mA/cm^2 for 24 h. The CH_4N_2S (1 g/L) was added in the solution as a hydrogen recombination poison. Platinum was used as an anode and the specimen was used as a cathode. In order to ensure that only the gauge section of the specimens was charged with hydrogen, the surfaces of the other parts were covered with paraffin.

* Corresponding author. Tel.: +86 29 82668695; fax: +86 29 82663453.
E-mail address: songxl@mail.xjtu.edu.cn (X. Song).

http://dx.doi.org/10.1016/j.msea.2014.07.085
0921-5093/

Table 1
Chemical composition of high strength steel (wt%).

Element	C	Si	Mn	P	S	Cr	Ni	Cu	Al	Fe
Analyzed	0.25	1.41	2.19	0.014	0.0049	1.07	0.011	0.018	0.015	Balance

Diffusible hydrogen concentration charged into the specimens was measured by the glycerol displacement method at 45 °C [14]. The charged specimens were removed from the charging cell, washed in water, dried and then immediately immersed in the bath filled with glycerol to release the hydrogen. This transition time was controlled to less than 2 min. The hydrogen releasing process was maintained for three days and the total hydrogen amount was determined from the volume of the displaced glycerol. The diffusible hydrogen concentration was calculated according to the following equation:

$$C_H = \frac{V}{m} \times 100 \quad (1)$$

where C_H (ml/100 g) is the diffusible hydrogen concentration, V (ml) is the hydrogen volume released from the specimen and m (g) is the weight of the gauge section of the specimen.

2.3. Electroplated cadmium

To prevent hydrogen releasing from the charged specimens, electroplated cadmium coating of about 15 μm thickness on the samples' surface is an effective way [15]. After hydrogen-charged, electroplated cadmium was carried out immediately. Protective cadmium plating was performed in an aqueous solution with 98% oil of vitriol (50 g/L), $CdSO_4$ powder (50 g/L), Na_2SO_4 (45 g/L), glutin (6 g/L) and phenol (3 g/L) at the current density of 25 mA/cm^2 for 5 min. The cadmium was used as an anode and the specimen was used as a cathode.

2.4. Slow strain-rate tensile

A typical stress–strain curve of the non-deformed sample is presented in Fig. 1. Tensile specimens were submitted to various degrees of tensile pre-strain from 0% to 7% at a nominal strain-rate of 2×10^{-4}/s, mechanically polished with #800 SiC girt paper. Some specimens were electrochemically hydrogen-charged. SSRT tests were performed on the pre-strained specimens with or without hydrogen at a strain-rate of 2×10^{-5}/s. The index of relative susceptibilities to hydrogen embrittlement (HEI) of various specimens at given pre-strain was determined by measuring the relative tensile strength loss, which can be expressed as

$$HEI\ (\%) = \frac{\sigma_0 - \sigma_H}{\sigma_0} \times 100\% \quad (2)$$

where σ_0 is the ultimate tensile strength of the hydrogen-free specimen and σ_H is the ultimate tensile strength of hydrogen-charged specimen at the same pre-strain. After tensile testing, the fracture surfaces were observed by scanning electron microscopy.

3. Results

3.1. Tensile test results

Typical stress–displacement diagrams for hydrogen-charged or hydrogen-free specimens with 0%, 3%, 5% and 7% pre-strain are shown in Fig. 2. For all hydrogen-free specimens the stress increased with displacement, reached ultimate tensile strength (UTS), decreased with further displacement and then the fracture occurred, as shown by the black line in Fig. 2, while all hydrogen-charged specimens fractured much earlier and showed obvious HE characteristic, as shown by the

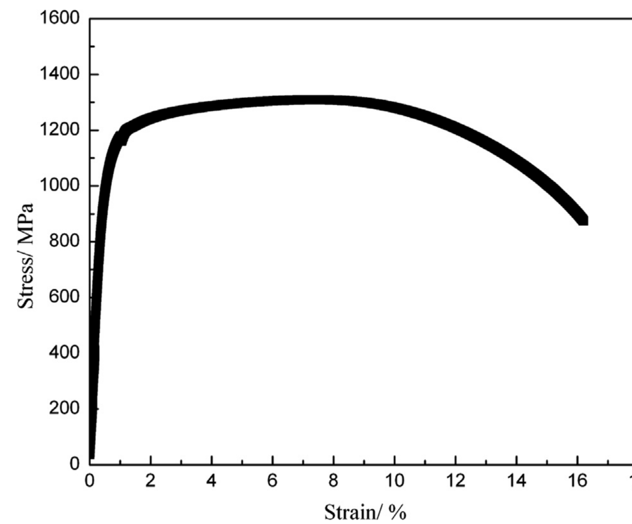

Fig. 1. Engineering stress–strain curve of the 0% pre-strain sample.

red line in Fig. 2. The relationship between UTS or UTS-H (UTS of the hydrogen-charged specimens) and pre-strain is shown in Fig. 3. As the pre-strain increased, UTS increased while UTS-H initially increased, reached maximum value at 3% pre-strain and dramatically decreased. Fig. 4 shows the elongation of the specimens as a function of pre-strain. It can be seen that the elongation of the hydrogen-charged specimens is much lower than that of hydrogen-free specimens, indicating significant losses in ductility due to hydrogen. And with increasing pre-strain, elongation of both hydrogen-charged and hydrogen-free specimens decreased. The HEI vs. pre-strain curves are displayed in Fig. 5. With increasing pre-strain, the HEI initially decreased and then increased.

3.2. Diffusible hydrogen concentration

The variation of diffusible hydrogen concentration with the pre-strain is shown in Fig. 6(a). With increasing pre-strain, the hydrogen concentration increased. At low pre-strain, the hydrogen concentration slightly increased. However, a large amount of hydrogen was introduced into the specimen at 7% pre-strain, reaching 23.54 ml/100 g. Meanwhile the amount of hydrogen was 11.78 ml/100 g at 0% pre-strain.

3.3. Fractography

The SEM fractographs for hydrogen-free or hydrogen-charged specimens with 0%, 3%, 5% and 7% pre-strain are shown in Figs. 7 and 8, respectively. In the case of hydrogen-free samples, the fracture surface showed many micro-voids with a range of sizes, including large and deep dimples, as shown in Fig. 7(a–d). For 0% pre-strain samples, many secondary cracks are easily observed in Fig. 7(a). In addition, few brittle-like features are observed on the fracture surface in Fig. 7(a–d).

However, for hydrogen-charged specimens with different pre-strains the fracture exhibited a mixed mode fracture of quasi-cleavage and intergranular fracture, accompanied by secondary crack, tearing ridge and micropores on the grain boundary, as shown in Fig. 8 (a–d), which are typical characteristics of HE [16]. It was reported by